

1 **Supplement:**

2

3 **No involvement of alveolar macrophages in the initiation of carbon nanoparticle induced**
4 **acute lung inflammation in mice**

5 Shanze Chen^{1, 2*}, Renfu Yin^{1, 3*}, Kathrin Mutze¹, Youjia Yu¹, Shinji Takenaka¹, Melanie
6 Königshoff¹, Tobias Stoeger^{1#}

7

8

9

10 **List of Additional Files:**

11

12 **Additional Methods:**

13 **Figure S1:** Ultrastructure of CNP-aerosols (A) and aqueous dispersion (B).

14 **Figure S2:** Enrichment of cell-specific gene expression in CD45- and CD45+ lung cells and
15 total BAL cells

16 **Figure S3:** Purity of isolated primary murine ATII cells.

17 **Figure S4:** Synopsis of gene expression results of all four cell isolation experiments

18 **Figure S5A:** Gene expression profile of BAL macrophages 3 and 12h after CNP and 12h
19 after LPS instillation

20 **Figure S5 B:** BAL neutrophil and macrophage numbers 3 and 12h after CNP and 12h after LPS
21 instillation

22 **Figure S6:** Detection of inflammatory cell activation by immunostaining, we used NFkB-GFP-
23 reporter mice

24 **Additional Reference**

25

26 **Additional Methods:**

27 **CNP generation**

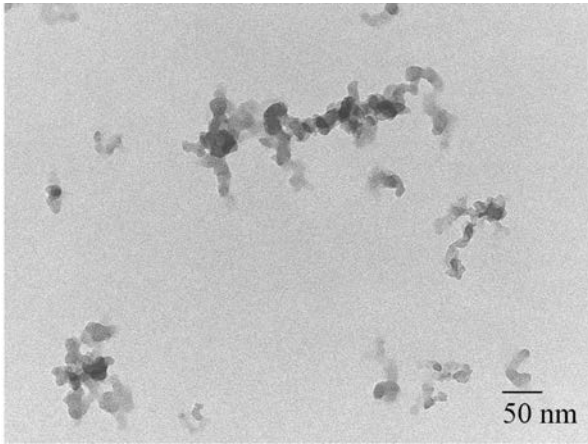
28 Particles were generated by the method described by Roth et al. 2004. The aerosol consists
29 of primary particles of 7-12nm diameter, forming agglomerates with an average number size
30 distribution of 48.9 ± 1.8 nm (equivalent mobility diameter) and a mean number
31 concentration of $7.7 \pm 0.86 \cdot 10^6 \text{ cm}^{-3}$ (Andre et al. 2006). According to the particle spectra,
32 92% of the generated particle agglomerates were nanoparticles ($<0.1 \mu\text{m}$). Airborne
33 particles were collected on $0.2 \mu\text{m}$ pore size polytetrafluorethylen (PTFE) filters (no. 11807–
34 50-N, Sartorius, Germany) using a vacuum pump, and removed from the filters using a
35 stainless steel spatula in a clean bench (Figure S1A). Particles were resuspended in water in
36 the same way as for the instillation procedure, mounted on the TEM-grids and analyzed by
37 transmission electron microscopy (TEM) as described previously (Stoeger et al. 2006). CNP
38 dispersions showed a mean agglomerate size of $0.19 \mu\text{m}$, measured by dynamic light
39 scattering (Malvern Zetasizer Nano ZS).

40 **Immunostaining**

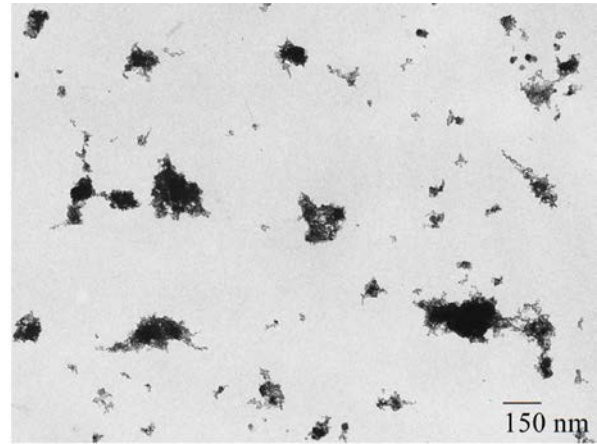
41 Briefly, lungs were embedded in paraffin and sectioned ($5 \mu\text{m}$). After deparaffinization
42 (xylene and gradual ethanol), slides were incubated in H_2O_2 buffer (40ml Methanol, 3ml 30%
43 H_2O_2 , 7ml dd H_2O) for 20 min at room temperature followed by antigen retrieval at 125°C for
44 15min. After blocking sections were incubated with rabbit polyclonal anti GFP antibody
45 (1:2000, ab290, Abcam, USA) at 4°C overnight and alkaline phosphatase conjugated goat
46 anti-rabbit IgG as secondary antibody at room temperature for 30min. Detection was done
47 using the Vulcan Fast Red Chromogen Kit 2 (901-FR805-080515, Biocare Medical, USA)
48 according to the manufacturer's instructions.

49 **Figure S1:**

50 **A**



B

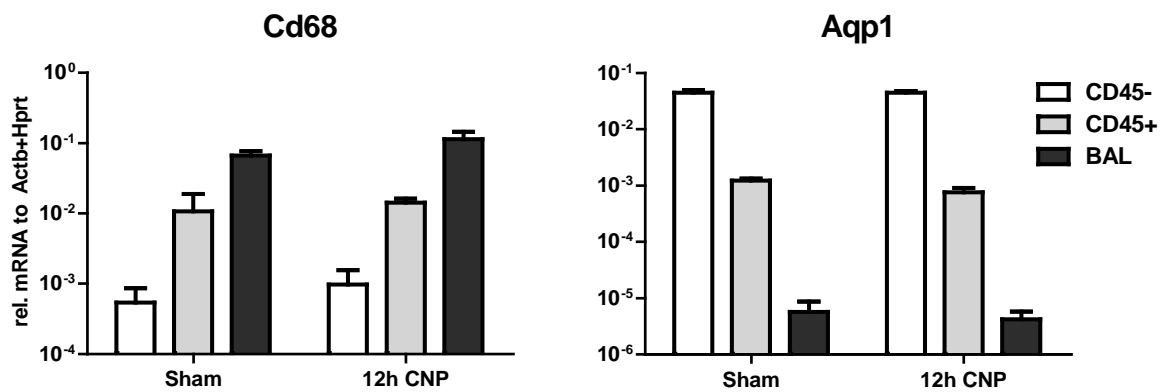


51

52 **Figure S1:** Ultrastructure of CNP-aerosols (A) and aqueous dispersion (B).

53

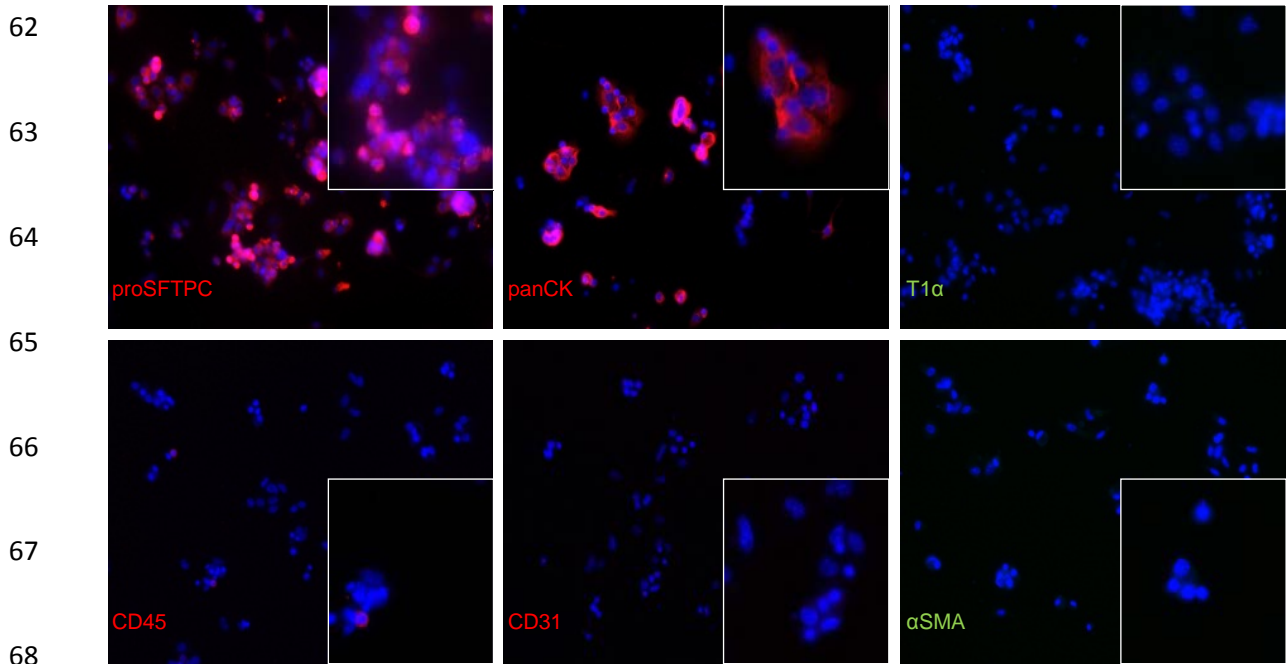
54 **Figure S2:**



55

56 **Figure 2S** shows the enrichment of macrophage-specific Cd68 and alveolar epithelial cell-
57 specific Aqp1 gene expression in CD45- and CD45+ lung cells and total BAL cells. Expression
58 levels are given at the log-10 scale, relative to Actb + Hprt. Results show means and SEM out
59 of 3 replicas and the expression pattern are representative for three independent
60 experiments.

61 **Figure S3**



69 **Figure S3:** Purity of isolated primary murine ATII cells. Immunofluorescence staining was
70 performed on primary murine ATII cells cultured on chamber slides over night for
71 assessment of purity. Fluorescent images represent a 200 x magnification, whereas image
72 inserts represent a 400 x magnification. Stainings are shown in red for the ATII cell marker
73 proSFTPC (pro surfactant protein C) and panCK (Pan Cytokeratin), the endothelial marker
74 CD31, and the leucocyte marker CD45, as well as in green for the ATI cell marker T1α
75 (podoplanin) and the fibroblast marker α-Sma (α-smooth muscle actin).

76

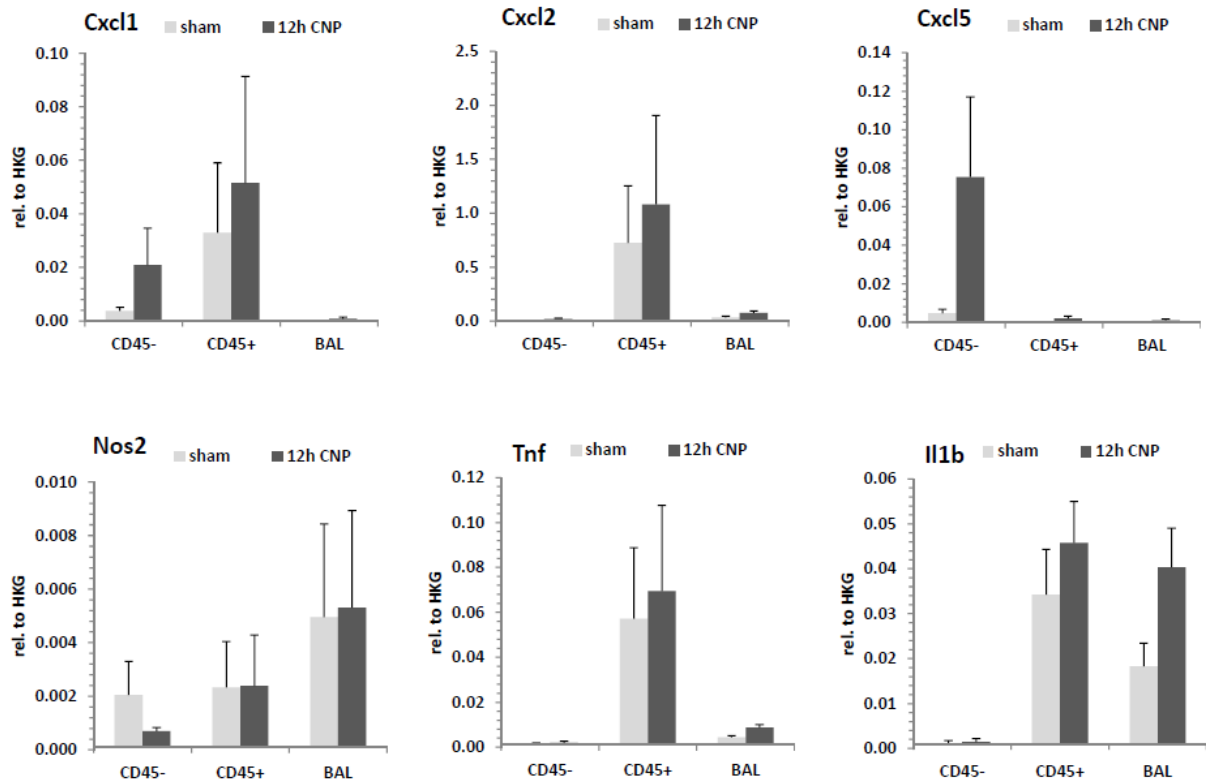
77

78

79

80

81 **Figure S4:**



82

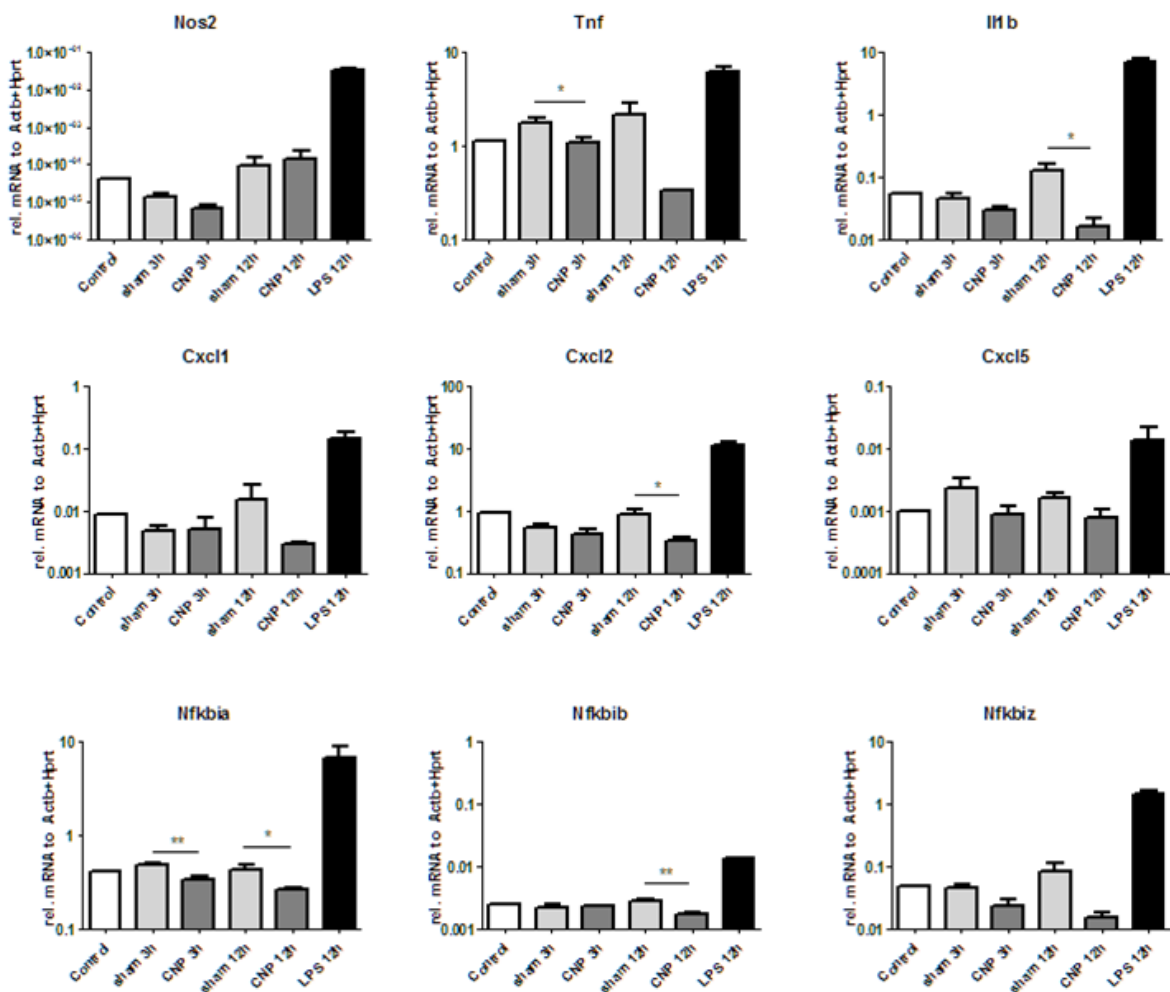
83 **Figure S4** shows a synopsis of the gene expression results from the four individual cell
 84 isolation experiments, of which one representative profile is given in figure 6. CD45-
 85 (alveolar epithelial cells), CD45+ leukocytes and total BAL cells were isolated from mice 12 h
 86 after the treatment with water (sham) or CNP. Expression levels are given relative to Actb +
 87 Hprt. Results show means and SEM out of four independent experiments.

88 Even if the inter-experimental variation of expression signals caused considerable standard
 89 errors which mask statistical significance, CNP triggered inductions still get evident for the
 90 genes Cxcl1 and -5. Note that the CNP exposure related changes for Tnf and Il1b expression
 91 in BAL cell isolates shown here, are absent in figure 5 where macrophages purified from BAL
 92 cells have been used (see METHODS: "Alveolar macrophages isolation"). Since limitations in
 93 BAL cell numbers did not allow for AM purification, the BAL cell expressions shown in Figure

94 S4 are besides alveolar macrophages also derived from neutrophil granulocytes, thereby
 95 distorting the macrophage related expression pattern shown in figure 5.

96

97 **Figure S5A**



98

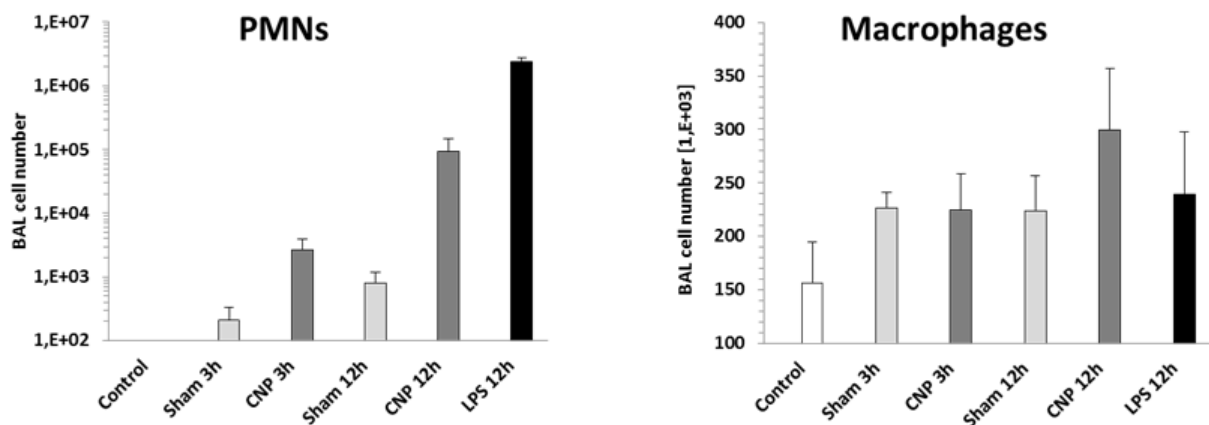
99 **Figure S5A** shows the gene expression profile of by BAL isolated and attachment purified
 100 macrophages, similar as investigated in Figure 5. In this independent round of experiment,
 101 mice were left untreated (control, n = 2), instilled with water (sham; n = 6), or again 20ug
 102 CNP (n = 6) or 0.1ug LPS (*E. coli* O55:B5, strain CDC 1644–70; n = 5) as positive control for
 103 macrophage activation. BAL was performed after 3 and 12h for the sham and CNP groups

104 and 12h for the LPS positive control. Gene expression is shown for of the macrophage
105 activation markers Nos2, Tnf and Il1b (upmost row), the chemokines Cxcl1, Cxcl2 and Cxcl5
106 (middle row) and the NF- κ B signaling pathway genes Nfkbia, Nfkbib and Nfkbiz (lowest row)
107 and presented relative to Actb & Hprt. Values are given as mean \pm SEM, asterisks represent
108 significance as compared to respective sham group with * $p < 0.05$, and ** $p < 0.01$.

109

110

111 **Figure S5B**



112

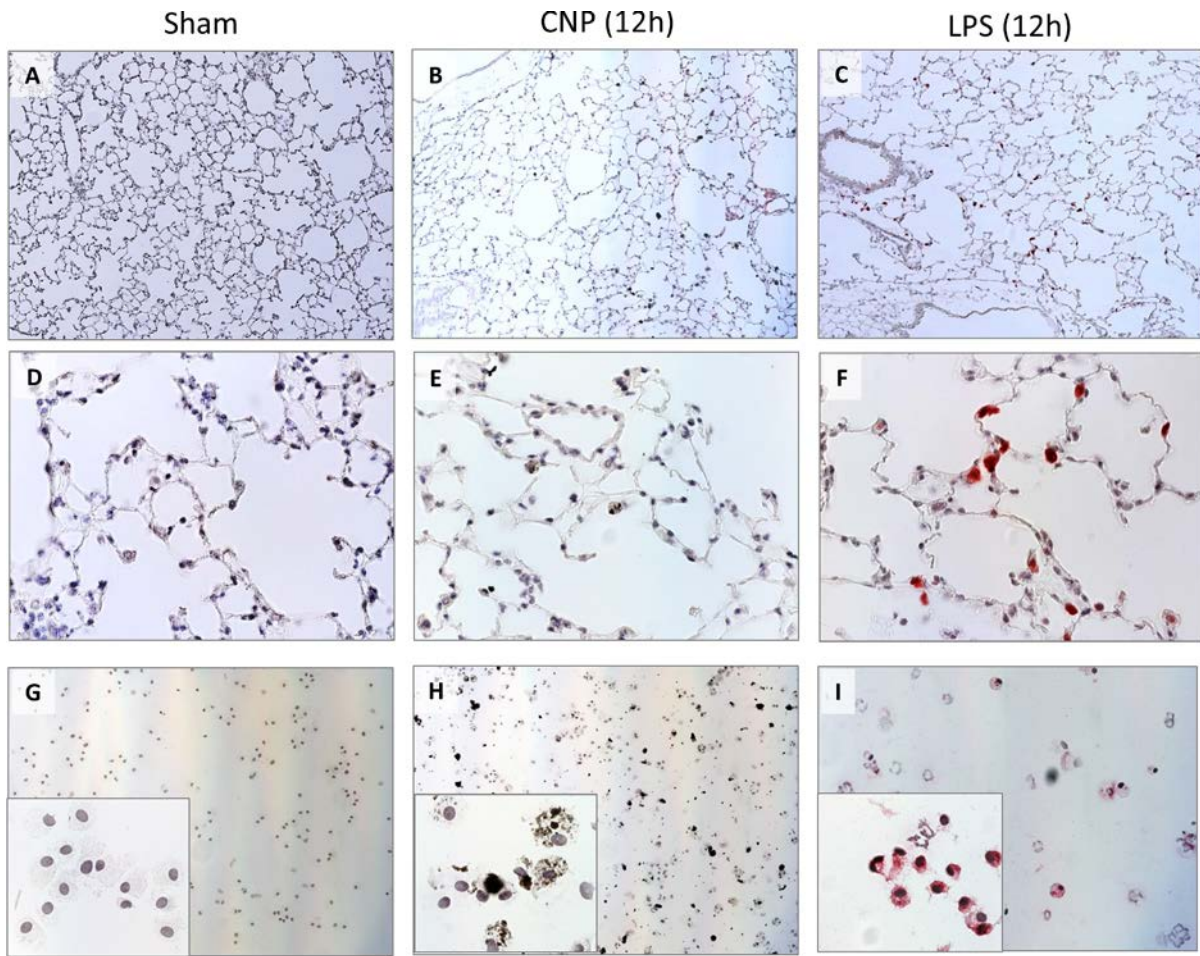
113 **Figure S5B** illustrates the inflammatory response, shown by the BAL neutrophil (PMN) and
114 macrophage numbers. Because of the wide spectrum of the inflammatory response, PMN
115 numbers are blotted at the logarithmic scale.

116

117

118

119



121

122 **Figure S6:** To detect inflammatory cell activation at the histological level by immunostaining,
 123 we used NFkB-GFP-reporter mice (cis-NF-kBEGFP, C57BL/6 strain, Magness et al. *J Immunol.*
 124 2004; three NF-kB cis elements drive enhanced GFP). The NF-kappa-B1 driven GFP-reporter
 125 protein was detected on PFA (4%) fixed lungs (A - F) or cytopsin (G - I) with the rabbit
 126 polyclonal anti-GFP antibody. Mice were intratracheally exposed to 50 ul water (sham: A, D,
 127 G), 20ug CNP (B, E, H) or 0.1ug LPS (C, F, I) for 12h. Figure S61 D, E and F show a 4 fold
 128 magnification of A, B and C. Immunostaining for the NFkB driven GFP-reporter protein shows
 129 a clear inflammatory activation of alveolar epithelial cells and macrophages (red staining) for
 130 the LPS exposed lungs and BAL macrophages, not seen in sham and CNP exposed animals.
 131 Images shown are representative for micrographs obtained from two different mice.

132 **Additional Reference:**

133 Magness ST, Jijon H, Van Houten Fisher N, Sharpless NE, Brenner DA, Jobin C. In vivo pattern
134 of lipopolysaccharide and anti-CD3-induced NF-kappa B activation using a novel gene-
135 targeted enhanced GFP reporter gene mouse. *J Immunol.* 2004 Aug 1;173(3):1561-70